

## Thermally stable electrostrains of morphotropic 0.875NaNbO<sub>3</sub>-0.1BaTiO<sub>3</sub>-0.025CaZrO<sub>3</sub> lead-free piezoelectric ceramics

He Qi, Ruzhong Zuo,<sup>a)</sup> Jian Fu, and Mengxian Dou

*Institute of Electro Ceramics and Devices, School of Materials Science and Engineering, Hefei University of Technology, Hefei, 230009, People's Republic of China*

(Received 6 January 2017; accepted 4 March 2017; published online 17 March 2017)

The 0.875NaNbO<sub>3</sub>-0.1BaTiO<sub>3</sub>-0.025CaZrO<sub>3</sub> relaxor ferroelectric ceramics were reported to exhibit thermally stable electrostrains (~0.15% @ 6kV/mm) from room temperature (RT) to ~175 °C and comparable strain hysteresis (<13%) to that of typical lead-based piezoelectric ceramics. Dominant strain contribution mechanisms with increasing temperature were analyzed by means of temperature-dependent permittivity, polarization, and strain measurements and synchrotron x-ray diffraction. The rhombohedral (R) and tetragonal (T) morphotropic phase boundary provided a solid structural base for temperature-stable piezoelectric strains from RT to ~140 °C. The growth of polar nanoregions (pseudocubic) into microdomains (R) and subsequent field-induced R-T phase transition, as well as large electrostrictive effects, sequentially contributed to high electrostrain levels in the proximity of the Curie temperature (from 140 to 175 °C). In addition, the observed low strain hysteresis was attributed to the small strain fraction from domain switching. These experimental results demonstrated that NaNbO<sub>3</sub>-based relaxor ferroelectrics might be potential lead-free materials for actuator applications. *Published by AIP Publishing.*  
[\[http://dx.doi.org/10.1063/1.4978694\]](http://dx.doi.org/10.1063/1.4978694)

Piezoelectric ceramics have been widely applied in ceramic actuators owing to their excellent electromechanical properties, particularly Pb(Zr,Ti)O<sub>3</sub>-based solid solutions lying a morphotropic phase boundary (MPB) between rhombohedral (R) and tetragonal (T) ferroelectric phases.<sup>1</sup> However, the use of lead-based ceramics has brought about serious concerns about the environmental pollution, and thereby, the development of lead-free piezoceramics has attracted much interest in the past few decades.

Until now, several typical lead-free material systems such as (Bi<sub>0.5</sub>Na<sub>0.5</sub>)TiO<sub>3</sub> (BNT)-,<sup>2-4</sup> BaTiO<sub>3</sub> (BT)-,<sup>5,6</sup> and (Na,K)NbO<sub>3</sub> (NKN)-<sup>7-9</sup> based lead-free ceramics have been extensively reported. Either limited piezoelectric coefficient values or poor temperature stability of piezoelectric properties has made these lead-free materials insufficient for ceramic actuators in service within a wide temperature range.<sup>10,11</sup> Large electrostrains up to ~0.4% were recently reported in BNT-based relaxor ferroelectric ceramics.<sup>12,13</sup> However, their strains displayed serious hysteresis (>65%), which limits their applications in actuators. Generally, strain hysteresis, which is mainly attributed to domain switching, can be influenced by the measurement conditions such as frequency and electric field because domain switching is the time and electric field-dependent nucleation and growth process of domains.<sup>14,15</sup> Purely electrostrictive lead-free relaxor ferroelectric ceramics are still limited by their relatively low strain values and particularly limited usage temperature ranges, even if a nearly hysteresis-free strain and a rapid response feature are involved.<sup>16-18</sup> Modified NKN-based lead-free piezoelectric ceramics usually exhibited temperature-dependent strains owing to the temperature-sensitive polymorphic phase

boundary (PPB) although diffuse phase transition (PPT) was believed to help improve the temperature stability to a certain degree.<sup>19</sup> The temperature stability of PPB-based lead-free ceramics can be optimized by shifting PPT temperatures below room temperature (RT), but their piezoelectric and electromechanical properties would be sacrificed.<sup>20</sup>

A morphotropic lead-free (0.9-x)NaNbO<sub>3</sub>-0.1BaTiO<sub>3</sub>-xCaZrO<sub>3</sub> ((0.9-x)NN-0.1BT-xCZ) ceramic has been recently reported to exhibit a vertical phase boundary and consequently temperature-insensitive piezoelectric properties at x = 0.025.<sup>21</sup> In this work, the strain characteristic of the x = 0.025 composition was explored as a function of temperature from RT to 180 °C. The underlying mechanism of generating thermally stable strains was clarified by means of *in-situ/ex-situ* synchrotron x-ray diffraction (XRD) in combination with temperature-dependent dielectric permittivity, polarization, and strain measurements.

The x = 0.025 NN-based lead-free ceramic was prepared by using a conventional solid-state reaction method. The detailed experimental procedure could be referred elsewhere.<sup>21</sup> Dielectric properties of virgin and poled samples as a function of temperature and frequency were measured by using an LCR meter. The quasi-static piezoelectric charge constant d<sub>33</sub> was measured by using a Berlincourt meter. The piezoelectric strain constant d<sub>33</sub> was obtained via dividing the maximum unipolar strain by the applied electric field magnitude on poled samples. The ferroelectric testing system (Precision multiferroic, Radiant Technologies Inc., Albuquerque, NM) connected with a laser interferometric vibrometer (SP-S 120, SIOS Meßtechnik GmbH, Germany) was used to measure strain versus electric field (S-E) curves at 10 Hz as a function of temperature. For XRD measurements, gold electrodes were sputtered onto both well-polished sides of the ceramic disk. High-resolution XRD measurements were taken at Shanghai

<sup>a)</sup> Author to whom correspondence should be addressed. Electronic mail: rzuo@hotmail.com, Tel: 86-551-62905285, Fax: 0086-551-62905285.

Synchrotron Radiation Facility (SSRF) using beam line 14B1 ( $\lambda = 1.2378 \text{ \AA}$ ).

Fig. 1(a) shows S-E loops (non-first cycle) of the  $x = 0.025$  ceramic as a function of temperature. It is evident that the unipolar strain ( $S_{\text{uni}}$ ) under  $6 \text{ kV/mm}$  ( $\sim 0.15\%$  at RT) first remained almost constant on heating till  $\sim 140^\circ\text{C}$  and then increased to a maximum value of  $\sim 0.16\%$  at  $150^\circ\text{C}$ . After that, it began to slightly decline but could still maintain a relatively high value before  $180^\circ\text{C}$ . In addition, all unipolar strain loops looked very slim, meaning a low strain hysteresis. The temperature-dependent relative strain and hysteresis values were compared with those of a few other lead-free ferroelectric ceramics,<sup>19,22–24</sup> as shown in Fig. 1(b). The strains of the  $x = 0.025$  ceramic in the studied temperature range were found to exhibit a lower hysteresis ( $< 13\%$ ), which was determined from the ratio of the widest part of the unipolar S-E loop over the maximum strain level. This value is much less than that of BNT-based relaxor ceramics<sup>12,13</sup> but is comparable with that of typical lead-based piezoelectric ceramics.<sup>25</sup> A small difference in the measurement frequency might have a little effect on the strain value and hysteresis but will not significantly change the above conclusion for these lead-free compositions. The frequency dependence of the strain hysteresis for the currently studied composition will be discussed infra. In addition, the strain values show a much better thermal stability, varying within  $\pm 10\%$  of its RT value. According to unipolar S-E loops, normalized strains ( $d_{33}^* = S_{\text{max}}/E_{\text{max}}$ ) were calculated at each temperature, as shown in Fig. 1(c). Compared with quasi-static  $d_{33}$ , high-field  $d_{33}^*$  did not decline in the proximity of the depolarization temperature  $T_d$  but maintained a high value up to  $180^\circ\text{C}$ . The quasi-static  $d_{33}$  values were almost temperature independent before  $T_d$  and then declined very rapidly. The temperature insensitive piezoelectric properties below  $T_d$  should be ascribed to the composition-axis vertical MPB between R and T phases.<sup>21</sup> Fig. 1(d) shows the dielectric permittivity ( $\epsilon_r$ ) and loss ( $\tan \delta$ ) values as a function of temperature for the virgin and poled  $x = 0.025$  ceramic. It is obvious that this sample exhibited a

typical dielectric relaxation behavior because of the dielectric diffuse phase transition and frequency dispersion. Below the temperature  $T_m$  at the dielectric maxima, another dielectric anomaly below  $T_m$  appeared after poling if one looked into the difference of  $\epsilon_r$ -T and  $\tan \delta$ -T curves before and after poling. This could be ascribed to the phase transition from the electric field induced long-range ferroelectric ordering back to ergodic polar nanoregions (PNRs) during heating. The temperature ( $T_{\text{fr}}'$ ) at the corresponding dielectric anomaly was about  $141^\circ\text{C}$ . As a consequence, the above mentioned depolarization process was attributed to the ferroelectric to relaxor phase transition instead of the ferroelectric to paraelectric phase transition. Therefore, for unpoled samples, ergodic PNRs at higher temperatures would spontaneously be frozen into nonergodic ones near  $141^\circ\text{C}$ . Moreover, it would be of much interest to note why strain values or  $d_{33}^*$  values could keep high levels above  $T_{\text{fr}}'$  and at even higher temperatures.

In order to further clarify the evolution mechanism of thermally stable electrostrains, the variation of (200), (220), and (222) diffraction lines at different temperatures for the  $x = 0.025$  sample at a virgin state ( $0 \text{ kV/mm}$ ), a poling state ( $6 \text{ kV/mm}$ ), and a poled state (poled under  $6 \text{ kV/mm}$  at the corresponding temperature) is shown in Fig. 2(a). Bipolar S-E loops (first cycle and non-first cycles) were measured to better understand the influence of external electric fields on the XRD lines, as shown in Fig. 2(b). Before  $150^\circ\text{C}$ , an irreversible R to T phase transition was induced by external fields. It can be noticed that the virgin sample should own an R-T phase coexistence in the temperature range from RT to  $\sim 140^\circ\text{C}$ .<sup>21</sup> After poling, all three diffraction lines demonstrated a pure T phase structure. This kind of irreversible R-T phase transition should also be responsible for the difference ( $S_{\text{ip}} = S_{\text{rem}} - S_{\text{neg}}$ ) between the negative strain  $S_{\text{neg}}$  and the remanent strain  $S_{\text{rem}}$  as indicated in Fig. 2(b). Moreover, the position and intensity of diffraction lines were found to vary if one compared the diffraction lines of poling and poled states (red and green lines in Fig. 2(a)), meaning the occurrence of lattice distortion and domain switching.

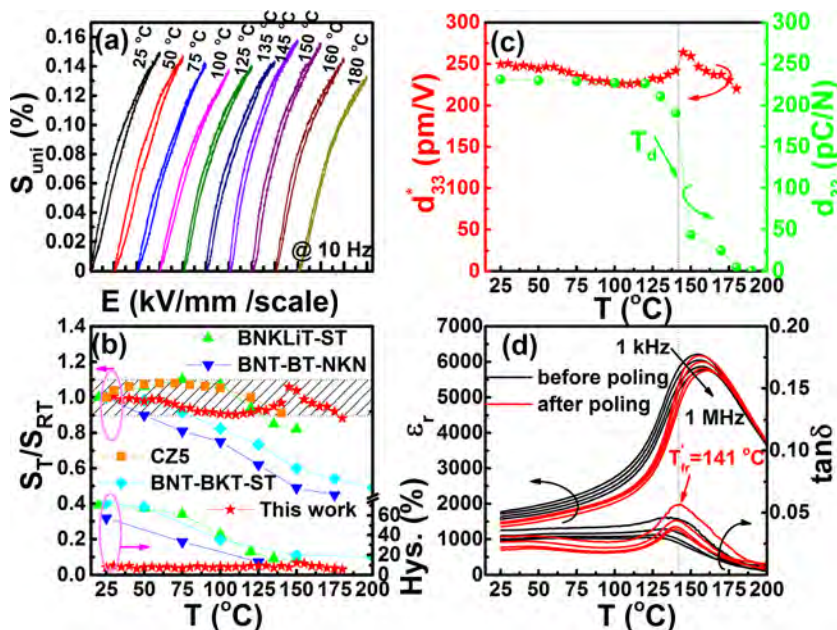


FIG. 1. (a) Unipolar strain of the  $x = 0.025$  ceramic under  $6 \text{ kV/mm}$  at different temperatures, (b) the variation of the strain value ( $S_T$ ) relative to their RT value ( $S_{\text{RT}}$ ) and the strain hysteresis (Hys.) as a function of temperature as compared with a few typical lead-free ferroelectric ceramics, (c) temperature-dependent quasi-static  $d_{33}$  and the normalized strain  $d_{33}^*$  of the  $x = 0.025$  ceramic, and (d) dielectric permittivity and loss tangent before and after domain switching as a function of temperature and frequency.

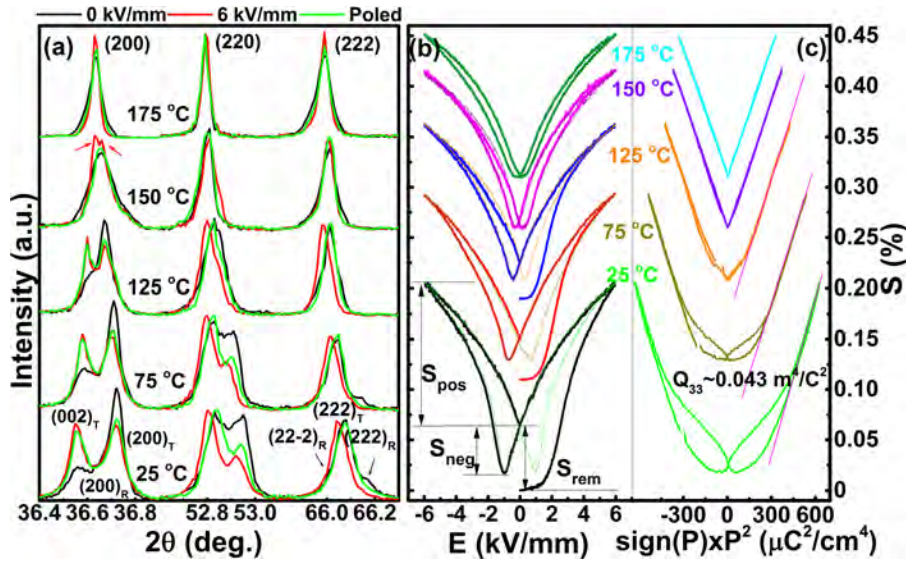


FIG. 2. (a) Evolution of synchrotron XRD patterns for the  $x=0.025$  ceramics at a virgin state (0 kV/mm), a poling state (6 kV/mm), and a poled state with varying temperatures, (b) bipolar strain curves measured from the first and non-first cycles for the  $x=0.025$  ceramic at various temperatures, and (c) strain versus the square of polarization ( $S$ - $P^2$ ) curves for the  $x=0.025$  ceramic measured at various temperatures.

At 150 °C, the virgin sample exhibited a pseudo-cubic (PC) phase structure as expected, which conforms to the fact that the sample is of ergodicity at this temperature (Fig. 1(d)). This PC phase transformed into a typical T phase structure under an electric field of 6 kV/mm, as characterized by the obvious peak splitting of (200) and (220). However, a PC structure was maintained after poling, indicating a reversible relaxor to ferroelectric phase transition. Under the application of an external electric field, ergodic PNRs were believed to first grow up such that ferroelectric microdomains with R symmetry can be detected. At even higher electric fields, an R to T phase structural transition was then driven, accompanying the domain switching, as highlighted by red arrows in Fig. 2(a). This is basically the reason for the generation of giant strains for a couple of relaxor ferroelectrics, although the strain magnitude of the  $x=0.025$  sample is not as large as that in BNT-based or Pb-based relaxors.<sup>12,13,26,27</sup>

With further increasing temperature up to the proximity of 175 °C, the PC (R) to T phase transformation was not observed any more, meaning that the field of 6 kV/mm is not high enough to overcome the energy barrier of the phase transition. However, the growth process of ergodic PNRs could be still confirmed if we looked into the variation of the diffraction peak widths at half height between samples of virgin and poling states, meaning that a PC ergodic state was driven into an R ferroelectric ordering state.<sup>21</sup> As a result of the coherence length of the x-ray, this process was usually considered as the growth of PNRs instead of a real phase transition.<sup>28</sup> That is to say, the ergodic PNRs should own an intrinsic R symmetry in this study. Moreover, because of the absence of domain switching, a relatively large strain at 175 °C should be ascribed to the polarization extension, behaving like a pure electrostrictive effect, as shown in Fig. 2(c). It can be seen that  $S$ - $P^2$  curves exhibited serious hysteresis at lower fields and nearly linear relationship at higher fields before 150 °C, which should be attributed to irreversible non-180° domain switching. Under a strong electric field, the domains could be clamped and the influence of domain switching would be eliminated, such that the linear increase in polarization merely originated from the ionic displacement. The slope of  $S$ - $P^2$  was used to determine the

electrostrictive coefficient  $Q_{33}$  according to the equation  $S_{33} = Q_{33} \cdot P_3^2$ . The result indicates that  $Q_{33}$  approximated to 0.043 m<sup>4</sup>/C<sup>2</sup>, almost independent of measuring temperature, which is nearly two times larger than those of Pb-based and Bi-based perovskite-structured ferroelectric ceramics.<sup>12,16,27</sup> A giant  $Q_{33}$  value and a high  $\epsilon_r$  value ( $\sim 6000$ , see Fig. 1) would enable a high-level low-hysteresis electrostrictive strain ( $\sim 0.15\%$ ). As the temperature is above 180 °C, the strain started to decline quickly although  $Q_{33}$  proved stable against temperature<sup>18,27</sup> because of a drastic drop of  $\epsilon_r$  (see Fig. 1(d)). In addition, because of the increased local random fields at higher temperatures, a long-range ferroelectric ordering or PNRs' growth can be hard to be induced so that the maximum polarization value became small.

It is known that the contribution of the converse piezoelectric effect and domain switching to strains can be quantitatively analyzed by means of XRD. The (200), (220), and (222) diffraction lines at RT for virgin, poling, and poled states of the  $x=0.025$  ceramic were fitted by using PeakFit software, as shown in Fig. 3(a). As discussed in Fig. 2(b),  $S_{rem}$  should be involved with all irreversible effects including irreversible R-T phase transition and irreversible non-180° domain switching, in which only the latter is correlated with  $S_{neg}$  as observed from  $S$ - $E$  curves of the non-first cycle. As a result, either  $S_{rem}$  or  $S_{neg}$  should not contribute to the positive strain ( $S_{pos}$ ), i.e., the  $S_{uni}$  value of the non-first cycle in Fig. 1(a). For normal ferroelectrics,  $S_{pos}$  should be a sum of intrinsic piezoelectric lattice strain ( $S_{lattice}$ ) and extrinsic reversible domain switching strain ( $S_{switch}$ ) ( $S_{pos} = S_{lattice} + S_{switch}$ ), in which  $S_{lattice}$  was calculated from a weighted average of the field-induced lattice strain  $S_{hkl}$  ( $\Delta d/d$ ) for individual  $hkl$  lattice planes.<sup>29</sup> In this case, the (220) and (222) reflections were taken into account. Moreover,  $S_{switch}$  was calculated according to the relationship between the variation of the volume fraction ( $f$ ) of domains parallel to the electric field and the  $S_{neg}$  value (Fig. 2(b)) using the following equation:  $S_{switch} = S_{neg} \cdot (f_{6kV/mm} - f_{poled}) / (f_{poled} - f_{virgin})$ .<sup>30</sup>

As shown in Fig. 3(b),  $S_{switch}$  was only  $\sim 0.0093\%$  ( $\sim 6.3\%$  of the  $S_{pos}$ ) at room temperature and showed little temperature dependence. It should be noted that  $S_{switch}$  in this study was significantly lower than that of typical PZT-,



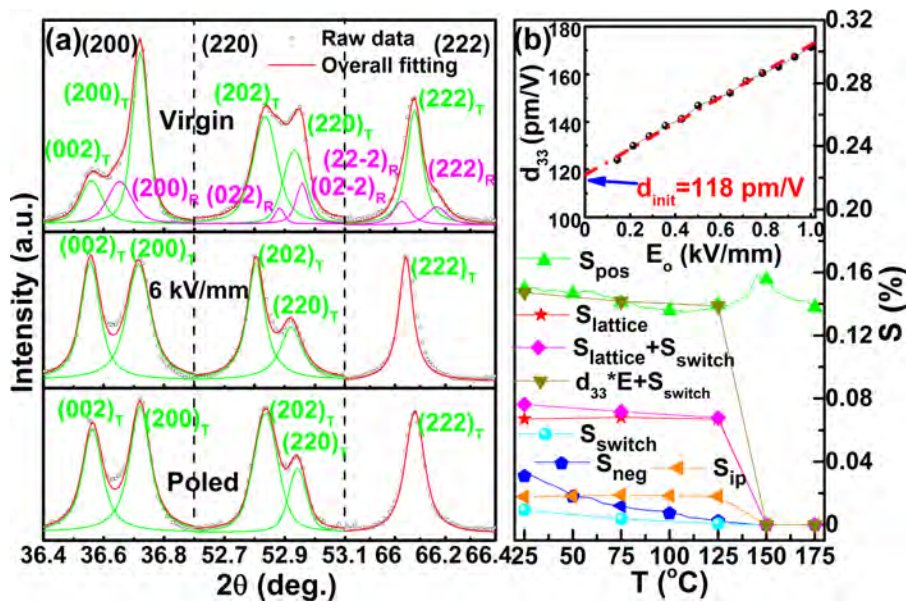


FIG. 3. (a) The (200), (220), and (222) diffraction peaks at RT for virgin, poling, and poled states of the  $x=0.025$  sample shown representatively and fitted by using PeakFit software as indicated and (b) temperature-dependent various strains  $S_{\text{pos}}$ ,  $S_{\text{neg}}$ ,  $S_{\text{ip}}$ ,  $S_{\text{switch}}$ ,  $S_{\text{lattice}}$ ,  $S_{\text{lattice}}+S_{\text{switch}}$ , and  $d_{33}^*E+S_{\text{switch}}$  of the  $x=0.025$  ceramic under 6 kV/mm. The inset shows the measured converse piezoelectric coefficient as a function of small-signal electric field magnitude at RT.

BNT-, and NKN-based compositions. This phenomenon should be attributed to the small lattice distortion of the studied composition<sup>21</sup> because the strain magnitude from domain switching generally depends on the degree of lattice distortion. The calculated tetragonality ( $c/a$ ) in the composition is only 1.0045, far below the values of other typical MPB compositions.<sup>30</sup> The extremely low  $S_{\text{switch}}$  would be the reason for the observed low strain hysteresis since it is mainly induced by domain switching. It is reasonable to expect that the strain hysteresis of the studied composition might show little frequency dependence. The strain response under a low electric field and in a wide frequency range will be investigated in detail in future. In addition, it is found that the calculated  $S_{\text{lattice}}$  ( $\sim 0.067\%$  at RT) was much larger than  $S_{\text{switch}}$  in this study. However, the calculated positive strain  $S_{\text{pos-cal}} (= S_{\text{lattice}} + S_{\text{switch}})$  is much smaller than the experimentally measured ones ( $S_{\text{pos}}$  in Fig. 2(b)), taking  $\sim 51\%$  of the total  $S_{\text{pos}}$  ( $\sim 0.15\%$  at RT). If the intrinsic strain contribution was evaluated using the product of quasi-static  $d_{33}$  and the applied electric field magnitude ( $E = 6$  kV/mm), the sum of  $d_{33}^*E$  and  $S_{\text{switch}}$  was found to approximate the  $S_{\text{pos}}$  value, meaning that the extrinsic strain contribution was seriously underestimated. The inset of Fig. 3(b) shows the converse piezoelectric coefficient  $d_{33}$  as a function of small-signal electric field magnitude. Below the coercive field, only intrinsic contribution and domain wall motion respond to the electric field, and thus nonlinear piezoelectric response obeys the Rayleigh relationship:  $d(E_0) = d_{\text{init}} + \alpha E_0$ , where  $d(E_0)$  is the strain coefficient at the applied electric field amplitude  $E_0$ ,  $d_{\text{init}}$  is the initial (zero field) piezoelectric coefficient, and  $\alpha$  is the piezoelectric Rayleigh coefficient.<sup>31</sup> A purely static  $d_{33}$  (i.e.,  $d_{\text{init}} = 118$  pm/V), which shows a good agreement with the  $S_{\text{lattice}}$ , can be obtained if we made an extrapolation up to zero field from the linear relation of  $d_{33}$  and  $E_0$ . In other words, a large extrinsic strain contribution from domain wall motion ( $\sim 49\%$ ) at lower fields was probably included in the measurement of quasi-static  $d_{33}$  ( $\sim 231$  pC/N at RT). In a word, temperature-insensitive intrinsic (lattice strain,  $\sim 47.9\%$ ) and extrinsic (domain wall motion,  $\sim 45.8\%$  and switching,  $\sim 6.3\%$ ) contributions are together responsible for

the thermal stability of strains in the temperature range from RT to  $T_d$ , which should be basically ascribed to the morphotropic nature of the phase boundary. This was further evidenced by the fact that  $S_{\text{ip}}$  was almost constant before  $T_d$  because it mainly depends on the relative content of R and T phases in the  $x = 0.025$  ceramic.

In summary, an electric field induced low-hysteresis ( $<13\%$ ) strain at 6 kV/mm varying within less than  $\pm 10\%$  of its RT value from RT to 175 °C was found in 0.875NN-0.1BT-0.025CZ lead-free ceramics. Such a strain characteristic was ascribed to the temperature-insensitive piezoelectric effect from RT to 140 °C, field induced PC ergodic relaxor to T ferroelectric phase transition near  $T_{\text{fr}}'$ , and pure electrostrictive effects above 175 °C. In addition, the low strain hysteresis, which can be comparable with that of some typical lead-based piezoelectric ceramics, was mainly attributed to the low strain contribution from domain switching. Synchrotron XRD results demonstrated a morphotropic nature of the phase boundary between R and T with an unchanged fraction of R and T below  $T_d$ , which basically contributed to the thermally stable piezoelectric contribution. Compared with intrinsic lattice contributions, a relatively large extrinsic strain contribution (domain wall motion and domain switching) was observed in the current study, taking  $\sim 52.1\%$  of the total  $S_{\text{pos}}$ . The enhancement of strains at higher temperatures was fundamentally attributed to the nature of relaxor ferroelectrics, which involved the growth of PNRs and subsequent R-T phase transition. The combination of an extremely large  $Q_{33}$  and a high dielectric response is responsible for large hysteresis-free electrostrictive strains. The temperature insensitivity and low hysteresis of large strains from RT to 175 °C indicated that the  $x = 0.025$  lead-free ceramic might have potentials in actuator applications.

This work was supported by the joint fund of National Natural Science Fund Committee and Large Devices of Chinese Academy of Science (U1432113) and the National Natural Science Foundation of China (51402079).

<sup>1</sup>B. Jaffe, W. R. Cook, and H. Jaffe, *Piezoelectric Ceramics* (Academic Press, New York, 1971).

- <sup>2</sup>T. Takenaka, K. I. Maruyama, and K. Sakata, *Jpn. J. Appl. Phys.* **30**, 2236 (1991).
- <sup>3</sup>H. Nagata, M. Yoshida, Y. Makiuchi, and T. Takenaka, *Jpn. J. Appl. Phys.* **42**, 7401 (2003).
- <sup>4</sup>X. X. Wang, X. G. Tang, and H. L. W. Chan, *Appl. Phys. Lett.* **85**, 91 (2004).
- <sup>5</sup>W. F. Liu and X. B. Ren, *Phys. Rev. Lett.* **103**, 257602 (2009).
- <sup>6</sup>M. Acosta, N. Novak, W. Jo, and J. Rödel, *Acta Mater.* **80**, 48 (2014).
- <sup>7</sup>Y. Saito, H. Takao, I. Tani, T. Nonoyama, K. Takatori, T. Homma, T. Nagaya, and M. Nakamura, *Nature* **432**, 84 (2004).
- <sup>8</sup>R. Z. Zuo and J. Fu, *J. Am. Ceram. Soc.* **94**, 1467 (2011).
- <sup>9</sup>X. P. Wang, J. G. Wu, D. Q. Xiao, J. G. Zhu, X. J. Cheng, T. Zheng, B. Y. Zhang, X. J. Lou, and X. J. Wang, *J. Am. Chem. Soc.* **136**, 2905 (2014).
- <sup>10</sup>H. Kungl and M. J. Hoffmann, *Acta Mater.* **55**, 5780 (2007).
- <sup>11</sup>C. A. Randall, A. Kelnberger, G. Y. Yang, R. E. Eitel, and T. R. Shrout, *J. Electroceram.* **14**, 177 (2005).
- <sup>12</sup>S. T. Zhang, A. B. Kounga, W. Jo, C. Jamin, K. Seifert, T. Granzow, J. Rödel, and D. Damjanovic, *Adv. Mater.* **21**, 4716 (2009).
- <sup>13</sup>J. G. Hao, B. Shen, J. W. Zhai, and H. Chen, *J. Appl. Phys.* **115**, 034101 (2014).
- <sup>14</sup>Y. H. Sin, I. Grinberg, I. W. Chen, and A. M. Rappe, *Nature* **449**, 881 (2007).
- <sup>15</sup>D. P. Chen and J. M. Liu, *Appl. Phys. Lett.* **100**, 062904 (2012).
- <sup>16</sup>C. Ang and Z. Yu, *Adv. Mater.* **18**, 103 (2006).
- <sup>17</sup>F. Li, L. Jin, and R. P. Guo, *Appl. Phys. Lett.* **105**, 232903 (2014).
- <sup>18</sup>R. Z. Zuo, H. Qi, J. Fu, J. F. Li, M. Shi, and Y. D. Xu, *Appl. Phys. Lett.* **108**, 232904 (2016).
- <sup>19</sup>F. Z. Yao, K. Wang, W. Jo, K. G. Webber, T. P. Comyn, J. X. Ding, B. Xu, L. Q. Cheng, M. P. Zheng, Y. D. Hou, and J. F. Li, *Adv. Funct. Mater.* **26**, 1217 (2016).
- <sup>20</sup>S. J. Zhang, R. Xia, and T. R. Shrout, *Appl. Phys. Lett.* **91**, 132913 (2007).
- <sup>21</sup>R. Z. Zuo, H. Qi, and J. Fu, *Appl. Phys. Lett.* **109**, 022902 (2016).
- <sup>22</sup>S. T. Zhang, A. B. Kounga, E. Aulbach, W. Jo, T. Granzow, H. Ehrenberg, and J. Rödel, *J. Appl. Phys.* **103**, 034108 (2008).
- <sup>23</sup>R. A. Malik, A. Hussain, A. Maqbool, A. Zaman, C. W. Ahn, J. U. Rahman, T. K. Song, W. J. Kim, and M. H. Kim, *J. Am. Ceram. Soc.* **98**, 3842 (2015).
- <sup>24</sup>K. Wang, A. Hussain, W. Jo, and J. Rödel, *J. Am. Ceram. Soc.* **95**, 2241 (2012).
- <sup>25</sup>H. Kungl, T. Fett, S. Wagner, and M. J. Hoffmann, *J. Appl. Phys.* **101**, 044101 (2007).
- <sup>26</sup>W. L. Zhao, R. Z. Zuo, J. Fu, X. H. Wang, L. T. Li, H. Qi, and D. G. Zheng, *J. Eur. Ceram. Soc.* **36**, 2453 (2016).
- <sup>27</sup>K. Uchino, S. Nomura, L. E. Cross, S. J. Jang, and R. E. Newnham, *J. Appl. Phys.* **51**, 1142 (1980).
- <sup>28</sup>R. Z. Zuo, F. Li, J. Fu, D. G. Zheng, W. L. Zhao, and H. Qi, *J. Eur. Ceram. Soc.* **36**, 515 (2016).
- <sup>29</sup>A. Pramanick, D. Damjanovic, J. E. Daniels, J. C. Nino, and J. L. Jones, *J. Am. Ceram. Soc.* **94**, 293 (2011).
- <sup>30</sup>H. Kungl, R. Theissmann, M. Knapp, C. Baetz, H. Fuess, S. Wagner, T. Fett, and M. J. Hoffmann, *Acta Mater.* **55**, 1849 (2007).
- <sup>31</sup>R. E. Eitel, T. R. Shrout, and C. A. Randall, *J. Appl. Phys.* **99**, 124110 (2006).